无 机 化 学 学 报

2018 年　　第 34 卷　　第 9 期

目　次

论　文

CHINESE JOURNAL OF INORGANIC CHEMISTRY

Vol.34 No.9 Sep. 2018

CONTENTS

Cover

Articles

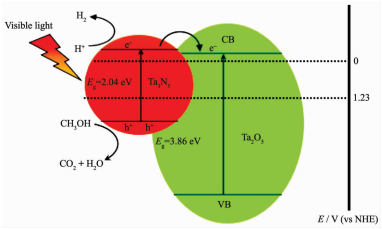

The formation of heterojunction structure for Ta_3N_5@Ta_2O_5 facilitated the rapid migration of photogenerated electrons by increasing the conduction band width of Ta5*d* orbits, and inhibited the recombination of photogenerated electrons and holes by the transfer from the conduction band of Ta_3N_5 to that of Ta_2O_5, then obviously enhancing the separation efficiency of charge carriers.

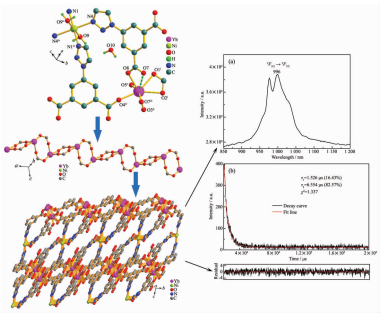

A series of 3D Ni(Ⅱ)-Ln(Ⅲ) heterometallic coordination polymers exhibit the characteristic luminescent emissions of the Ln(Ⅲ) in the visible and near infrared region with the long lifetime.

Preparation and Photothermal Catalytic Properties of Gold Nanospheres and Nanorods

LI Jian, WANG Jing-Hua, YANG A-Long,
SHI Zhen-Ning, WANG Jiang-Wei,
ZHAO Qin-Fu, ZHANG Ying

DOI:10.11862/CJIC.2018.189
Chinese J. Inorg. Chem., **2018**,**34**(9):1610-1614

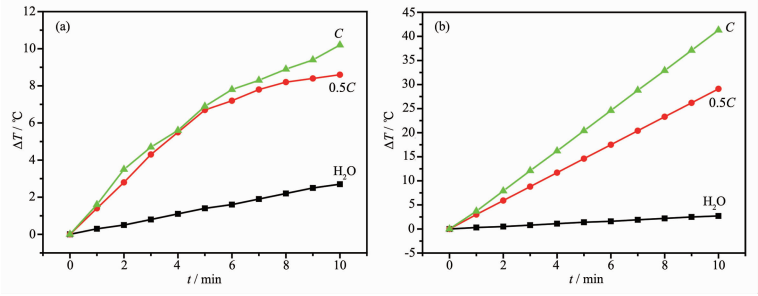

The gold nanospheres and nanorods (R=3.01) were synthesized, which show good performance on photothermal and catalytic behaviors.

Effect of Extraction Temperature on Hyper-coal Structure and Electrochemistry of Coal-Based Activated Carbon

GUO Bing-Lin, HOU Cai-Xia, FAN Li-Hua,
SUN Zhang

DOI:10.11862/CJIC.2018.201
Chinese J. Inorg. Chem., **2018**,**34**(9):1615-1624

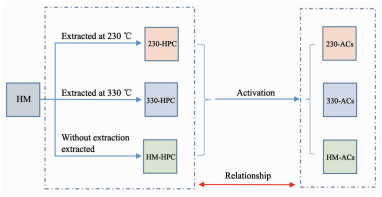

Different activated carbons were prepared by diverse hyper-coal extracted in different temperatures. The relationship is discussed between the functional groups in hyper-coal and the pore structure as well as electrochemical performance of the activated carbon.

Influences of Co^{2+} Doping Ratio on the Thermochromic and Variable Emissivity Properties of ZnO

XU Chen, FANG Gang, LIU Chu-Yang,
XU Guo-Yue, ZHU Yong-Mei, ZHANG Yan-Ting

DOI:10.11862/CJIC.2018.203
Chinese J. Inorg. Chem., **2018**,**34**(9):1625-1631

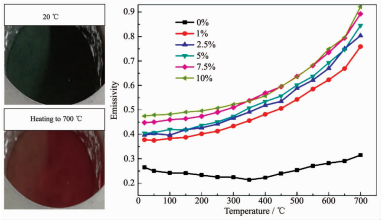

With testing temperature increasing from room temperature to 700 ℃, the ZnO powders doped by Co^{2+} ions change reversibly from green to tawny. Meanwhile, the emissivity increases gradually, and the maximum variation reaches 0.447.

Synthesis and Photocatalytic Degradation Performance for Rhodamin B of Zn-Cr-Cu Composite Metal Oxides Derived from Layered Double Hydroxides

MENG Yue, XIA Sheng-Jie, XUE Ji-Long,
NI Sheng-Liang, NI Zhe-Ming

DOI:10.11862/CJIC.2018.208
Chinese J. Inorg. Chem., **2018**,**34**(9):1632-1640

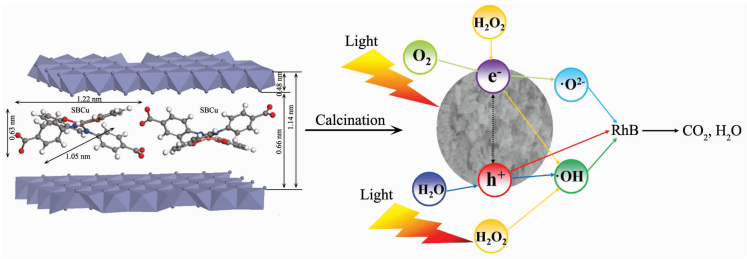

Zn-Cr-Cu composite metal oxides derived from hybrid Layered double hydroxides as a novel photocatalytic material exhibits a better photocatalytic activity for RhB degradation under the synergistic effect of H_2O_2.

Controlled Preparation and Performance Optimization of $Na_3V_2(PO_4)_2O_2F$ as Cathode Material for Sodium Ion Batteries

GU Zhen-Yi, GUO Jin-Zhi, YANG Yang, LÜ Hong-Yan, ZHAO Xin-Xin, XI Xiao-Tong, HE Xiao-Yan, WU Xing-Long

DOI:10.11862/CJIC.2018.204
Chinese J. Inorg. Chem., **2018**,**34**(9):1641-1648

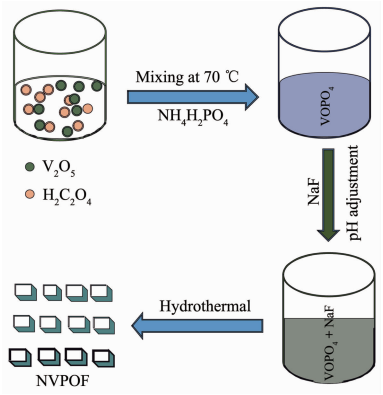

A simple hydrothermal preparation method was developed, regulating the morphology and size of the NVPOF by adjusting the key parameters including the pH value and hydrothermal temperature. The optimized NVPOF material exhibits the highest particle-size uniformity and there by the best electrochemical properties.

Design, Syntheses and Anticancer Activities of Platinum(Ⅳ) Prodrugs with Dihydrogen Phosphate as an Axial Ligand

GAO An-Li, XIONG Qing-Feng, JIANG Jing, YU Juan, LOU Li-Guang, LIU Wei-Ping

DOI:10.11862/CJIC.2018.211
Chinese J. Inorg. Chem., **2018**,**34**(9):1649-1654

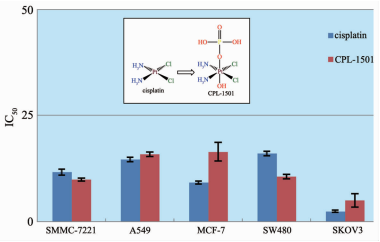

CPL-1501 is a platinum (Ⅳ) prodrug of cisplatin. With dihydrogen phosphate as an axial ligand, it has superior water-solubility and aqueous stability over cisplatin. It also displays comparable anticancer activity to cisplatin.

Seed-Layer Effect on Highly Oriented ZnO Nanorod Array Fabrication

ZHOU Fei-Chi, YUAN Long, FENG Shou-Hua, Martyn A McLachlan, ZHANG Jia-Qi

DOI:10.11862/CJIC.2018.210
Chinese J. Inorg. Chem., **2018**,**34**(9):1655-1662

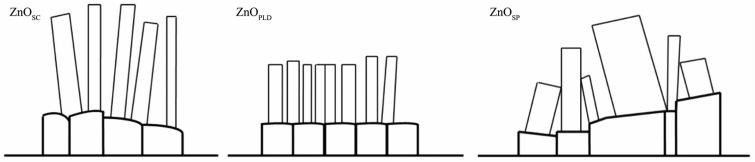

The ZnO nanorods exhibit strong substrate-dependent properties. The crystal orientation, surface roughness and grain size of the seed layers are key factors to control the nanorod growth.

Fabrication and Properties of Metal-Organic Framework@Mesoporous Composites

MA Miao-Miao, LI Mei, KE Fu-Sheng

DOI:10.11862/CJIC.2018.176
Chinese J. Inorg. Chem., **2018**,**34**(9):1663-1669

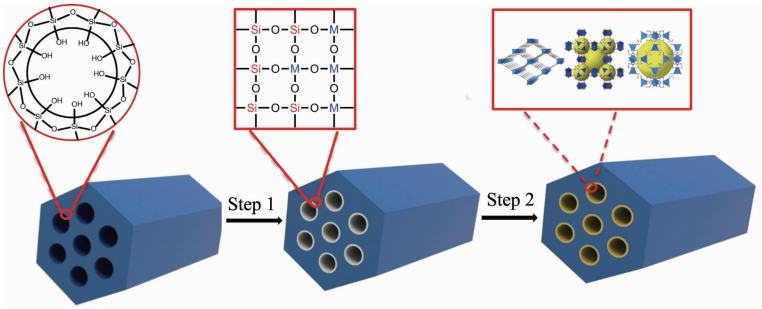

MOF@SBA-15 hierarchical structure is obtained by inclusion of metal oxide in the meso-pore of SBA-15 and in situ conversion of metal oxides to MOFs.

Fabrication and Electrochemical Performance of Mesoporous α-Fe_2O_3 Anodes for Lithium and Sodium Ion Batteries

LI Hua-Mei, CHEN Yu-Jie, ZHAO Xiao-Hui, DENG Zhao

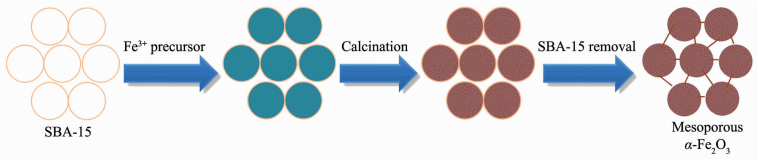

The highly ordered mesoporous α-Fe_2O_3 synthesized with SBA-15 as hard template in this work greatly promotes the electrolyte wettability and accommodates the volume expansion, and thus delivered high specific capacity both in lithium ion and sodium ion batteries.

DOI:10.11862/CJIC.2018.221
Chinese J. Inorg. Chem., **2018**,**34**(9):1670-1676

CN_x Nanotube Support Platinum-CeO_x as Highly Stable and Efficient Electrocatalyst for Oxygen Reduction Reaction (English)

FU Yu, AO Hong-Liang, ZHANG Ling-Xiao, GUO Yu-Meng, LIANG Ju-Mei, ZHANG Li-Juan, LI Fan

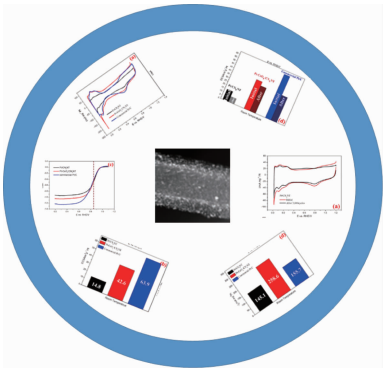

The as-prepared Pt-CeO_x/CN_xNT catalyst showed superior ORR activity, which is attributed to the existence of CeO_x, pyridine-like nitrogenin support and the unique hollow tube nanostructure of CN_xNT support. Moreover, the presence of CeO_x can significantly enhance the durability for both Pt nanoparticles and support.

DOI:10.11862/CJIC.2018.206
Chinese J. Inorg. Chem., **2018**,**34**(9):1677-1687

Controllable Fabrication of Mono-Shelled Hollow Sphere $CaCO_3$ Microspheres via CO_2 Bubbling Method: Potential Dye Carrier for Cell Bio-imaging (English)

LIU Jiang, SHA Feng, YANG Ting-Yu, MA Liang, ZHANG Jian-Bin

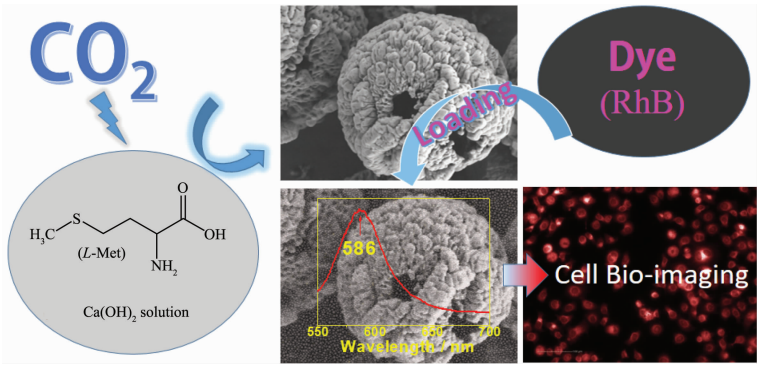

DOI:10.11862/CJIC.2018.220
Chinese J. Inorg. Chem., **2018**,**34**(9):1688-1700

Simple Way to Enhance the Photocatalytic Activity and Application in Antireflective Coatings for Amorphous TiO_2 (English)

LI Yuan-Yang, YAN Liang-Hong, JIANG Bo

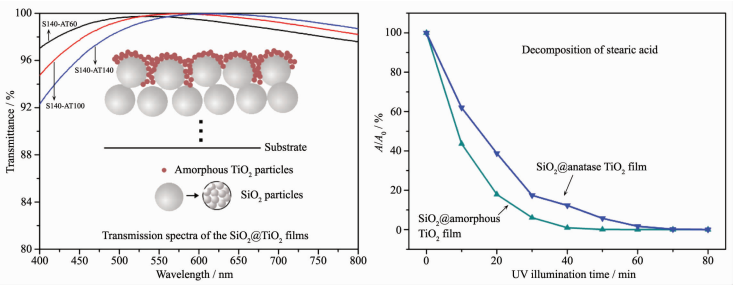

The SiO_2&amorphous-TiO_2 anti-reflective films show an exceptional photocatalytic activity even higher than the counterparts with anatase phase.

DOI:10.11862/CJIC.2018.205
Chinese J. Inorg. Chem., **2018**,**34**(9):1701-1709

Ti^{4+} Doped Perovskite for Efficient Perovskite Solar Cells by Grain Boundary Passivation (English)

TIAN Hui, XIONG Qi, LIU Peng, ZHANG Jing, HAN Lei, ZHANG Yu-Hao, ZHENG Yong-Jin, WU Li-Shuang, ZHU Yue-Jin

DOI:10.11862/CJIC.2018.200
Chinese J. Inorg. Chem., **2018**,**34**(9):1710-1718

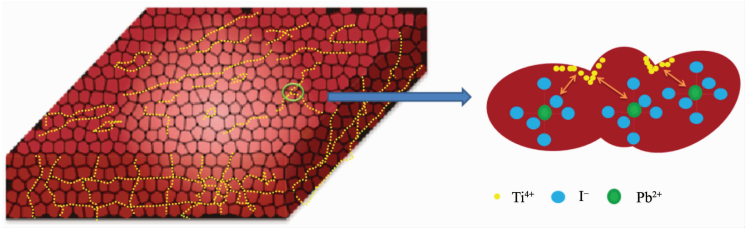

Ti^{4+} formed at the grain boundary to passivate the defects of polycrystalline perovskite film. The performance of perovskite solar cells is effectively improved.

Cu(Ⅰ)Fe(Ⅱ) Heterobimetallic Complexes Based on Functionalized 6-Methoxycarbonyl-2,2′-bipyridine Ligands (English)

HUANG Rong, ZENG Xue-Hua, WANG Wan-Man, ZHANG Meng-Li, CHEN Jing-Lin, LIAO Jin-Sheng, LIU Sui-Jun, WEN He-Rui

DOI:10.11862/CJIC.2018.188
Chinese J. Inorg. Chem., **2018**,**34**(9):1719-1724

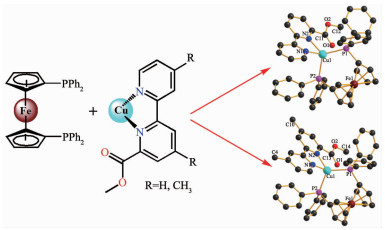

The introduction of 1,1′-bis(diphenylphosphino)ferrocene has a significant influence on luminescence properties of Cu(Ⅰ) complexes, which leads to the quenching of the potentially luminescent MLCT state of Cu(Ⅰ) species.

Two Binuclear Cu(Ⅱ) Complexes of Reduced Schiff Base Ligand Containing Benzimidazole Ring: Syntheses, Structures and Electrochemical Properties (English)

ZHAO Hai-Yan, LI Na, YANG Xiao-Dong

DOI:10.11862/CJIC.2018.218
Chinese J. Inorg. Chem., **2018**,**34**(9):1725-1732

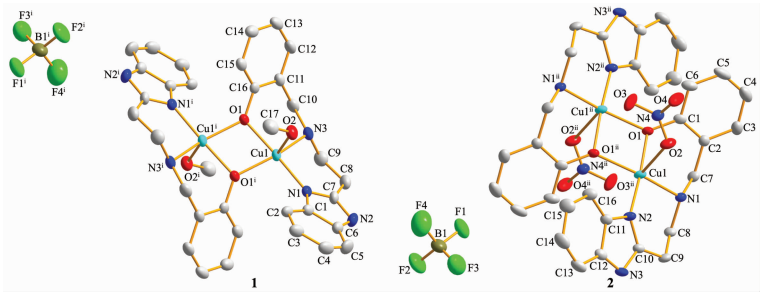

In the two complexes $[CuL(CH_3OH)]_2(BF_4)_2$ (**1**) and $[CuL(NO_3)_2]_2$ (**2**), each Cu(Ⅱ) cation adopts a distorted square pyramid arrangement with the Addison parameters (τ) of 0.31 and 0.35 for **1** and **2**, respectively. The electrochemical studies of **1** and **2** show two quasi-reversible one electron reduction processes.

Syntheses, Characterization and Luminescent Properties of Two Silver(Ⅰ) Complexes Based on N-donor and P-donor Ligands (English)

KUANG Xiao-Nan, WANG Yu, ZHU Ning, LIU Min, YANG Yu-Ping, LI Zhong-Feng, HAN Hong-Liang, JIN Qiong-Hua

DOI:10.11862/CJIC.2018.193
Chinese J. Inorg. Chem., **2018**,**34**(9):1733-1738

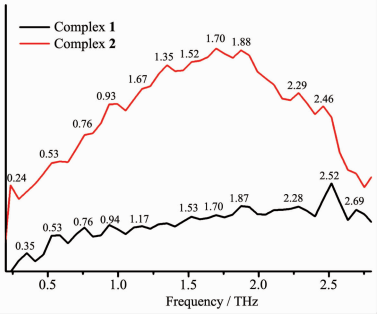

Both complex **1** and complex **2** are binuclear complexes. In complex **2**, the C–H···N intramolecular hydrogen bonds and the intramolecular C–H···π forces are observed. The room temperature terahertz (THz) absorption spectra of complexes **1** and **2** were measured in the range of 0.2~2.8 THz.

Crystal Structures and Fluorescence Properties of Cu(Ⅱ)/Ni(Ⅱ) Complexes with 4-(1,2,4-Triazol-1-yl)phenol Ligand (English)

ZHAO Hong-Kun, DING Bo, WANG Xiu-Guang, JIA Fang, YANG En-Cui, ZHAO Xiao-Jun

DOI:10.11862/CJIC.2018.219
Chinese J. Inorg. Chem., **2018**,**34**(9):1739-1746

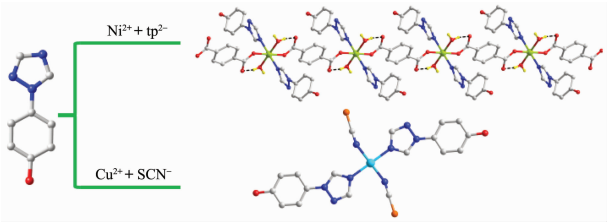

Assembly and Properties of a 2D Layer Coordination Polymer Containing Linear Tetranuclear Cobalt-Cluster Unit Bridged by Tricarboxylic Acid Ligand (English)

WANG Peng-Fei

DOI:10.11862/CJIC.2018.207
Chinese J. Inorg. Chem., **2018**,**34**(9):1747-1752

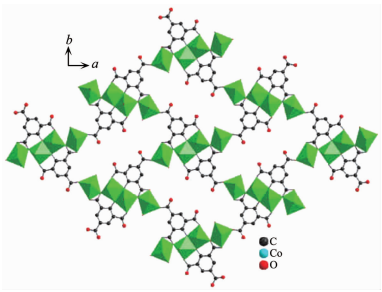

A 2D layer coordination polymer $[Co_2(O\text{-}BTC)(H_2O)_5]_n$ (**1**) has been constructed from a tricarboxylic acid ligand 2-hydroxyl-1,3,5-benzenetricarboxylic acid (HO-H_3BTC). Magnetic studies for compound **1** shows an antiferromagnetic interaction between the adjacent Co(Ⅱ) centers.

Preparation and Properties for Aza-Micheal Addition Reaction of Magnetic Y-MOF@SiO_2@Fe_3O_4 Catalysts (English)

MU Jin-Cheng, JIANG Sai, JI Sheng-Fu

DOI:10.11862/CJIC.2018.209
Chinese J. Inorg. Chem., **2018**,**34**(9):1753-1760

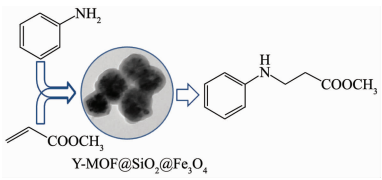

The catalyst performance of a core-shell magnetic Y-MOF@SiO_2@Fe_3O_4 catalyst for Aza-Micheal addition reaction with aniline and methyl acrylate was evaluated, and exhibited good reusability and good superparamagnetism.

Synthesis, Structure and Magnetic Property of Dysprosium(Ⅲ) Complex Based on β-Diketonate and Tetramethylimidazolium Ligands (English)

GE Jing-Yuan, CHEN Zhong-Yan, MA Jian-Ping, HUANG Shuai, DU Jia, WANG Hai-Ou, SU Kun-Peng, WANG Hai-Ying

DOI:10.11862/CJIC.2018.202
Chinese J. Inorg. Chem., **2018**,**34**(9):1761-1767

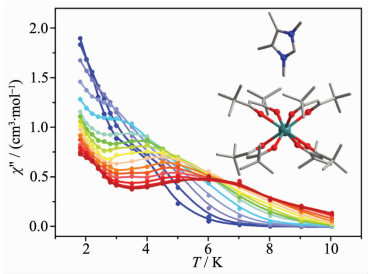

In the mononuclear dysprosium(Ⅲ) complex, the Dy(Ⅲ) ion locates in an approximately ideal D_{4d} coordination geometry, and each mononuclear $[Dy(thd)_4]^-$ anions is separated by $Tmim^+$ cations regularly with the shortest Dy ⋯ Dy distance of 1.229 8 nm. Complex **1** exhibits a field-induced single-ion magnetic behavior.

Syntheses, Crystal Structures and Luminescent Properties of Dinuclear d^{10} Complexes Based on a Ligand Formed *in Situ* by 8-Hydroxyquinoline (English)

GAO Xiang, XU Wei, WU Chang-Li, ZHU Xi-Miao, OU Yong-Cong, WU Jian-Zhong

DOI:10.11862/CJIC.2018.213
Chinese J. Inorg. Chem., **2018**,**34**(9):1768-1774

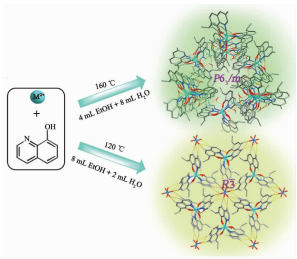

In situ synthesis and characterization of structures with different stacking for positive charged $[M_2(HL)_3]^+$ units have been reported here and showed that different lattice packing could affect the luminescent properties. Furthermore, the *in situ* synthetic organic ligand has been successfully extracted and characterized.